Dicopper(II) Complexes of a Binucleating N_4 Macrocycle containing Mono- and Di-atomic Bridges; Magnetic Interactions mediated by Alkoxo- and Diaza-bridging Ligands. Crystal Structures of $[Cu_2(L^1)(pz)_2][ClO_4]_2$, $[Cu_2(L^1)(OEt)_2(NCS)_2]$, and $[Cu_2(L^1)(OMe)_2(MeCN)_2][BPh_4]_2$†

Michael G. B. Drew * **and Paul C. Yates**
Department of Chemistry, The University, Reading, RG6 2AD
Ferida S. Esho, Jadwiga Trocha-Grimshaw, Aidan Lavery, Kieran P. McKillop, and S. Martin Nelson
Department of Chemistry, Queens University, Belfast BT5 5AC
Jane Nelson *
The Open University, 40 University Road, Belfast 7

Dicopper(II) complexes of 20-membered N_4 binucleating macrocycles L^1—L^3 derived by a cyclic [2 + 2] condensation of diformylthiophene or diformylfuran with the appropriate diamine have been synthesised and characterised by analytical, spectroscopic, magnetic, and *X*-ray diffraction methods. A pair of bridging ligands, either alkoxo, OR^- (R = H, Me, or Et), or diaza (pyrazolate or 1,2,4-triazolate), links the Cu^{II} ions. The crystal structure of three compounds $[Cu_2(L^1)(pz)_2][ClO_4]_2$ (**1**), $[Cu_2(L^1)(OEt)_2(NCS)_2]$ (**6**), and $[Cu_2(L^1)(OMe)_2(MeCN)_2][BPh_4]_2$ (**7**) have been determined by *X*-ray diffraction (Hpz = pyrazole). In structures (**6**) and (**7**) the copper(II) ions have a trigonal-bipyramidal environment, with ethoxy [(**6**)] or methoxy [(**7**)] bridges in a position axial to one Cu^{II} and equatorial to the other. Despite the parallel disposition of the d_{z^2} magnetic orbitals, strong antiferromagnetic superexchange is observed for this and the other parallel-planar alkoxo-bridged dimer described. In structure (**1**), the copper co-ordination environment is square planar, with *cis* disposed pyrazolate bridges. Moderate antiferromagnetic exchange is present in (**1**) and the other diaza compounds, and well defined triplet e.s.r. spectra are observed.

The synthesis of binuclear complexes where the metal ions are in close proximity remains an important objective of transition-metal and bioinorganic chemistry. The study of magnetic interactions between such closely spaced paramagnetic centres is currently receiving some attention, directed at identification of the factors which determine the nature and strength of the interactions. In many of the dimers studied to date, the internuclear separation and geometry are dictated by the bridging ligand which is in fact responsible for assembly of the dimer; with binucleating macrocyclic ligands however, this limitation need not apply. The macrocyclic donors fix the metal ions, and this determines, within the limits of the macrocycles flexibility, the internuclear distance. The co-ordination geometry, and hence the disposition of the bridging ligands is also determined by the macrocycle. In some cases,[1] a bridging donor can be incorporated into the macrocyclic skeleton (an endogenous bridge), but in the systems studied here there is no endogenous bridge, which allows for the insertion of a variety of exogenous bridging ligands. This permits a study of structure/function relationships over a range of internuclear separations and geometries unimpeded by constraints determined either by endogenous or exogenous bridges.

The ligands described in the present study are 20-membered binucleating macrocycles whose small cavity size encourages the incorporation of single-atom bridges between metal ions co-ordinated by the bis(imino) donors.[2] This preference for the monatomic bridge is demonstrated in the appearance of the rare single-atom bridging modes > SCN[3] or > NCS[4] of thiocyanate ion and the unusual 1,1-bridging mode of azide[4] in dimeric transition-metal complexes of L^1. In addition, an exceptionally large number of hydroxo- and alkoxo-bridged dimers are readily formed using this macrocyclic system. The magnetic properties of the bridged dicobalt(II) complexes have been described earlier;[4] in this paper we describe the analogous dicopper(II) complexes. We report here on the synthesis, properties, and structural characterisation of a series of dicopper complexes of the macrocycles L^1, L^2, and L^3, having a 20-membered inner large ring, the copper ions being bridged either by monatomic μ-alkoxo- or by diatomic 1,2-diaza- ligands.

Results and Discussion

Synthesis of the Dicopper(II) Complexes.—The macrocycles L^1 and L^2 were assembled by template synthesis on Group 2 metals using the appropriate diamine and dialdehyde. The

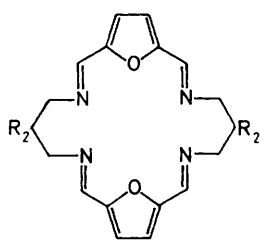

L^1 R = H
L^2 R = CH_3

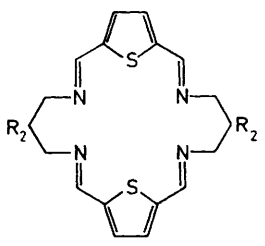

L^3 R = H

† (23,24-Dioxa-3,7,14,18-tetra-azatricyclo[18.2.1.1^{9,12}]tetracosa-1(22),2,7,9,11,13,18,20-octaene)-di-μ-pyrazolato-dicopper(II) perchlorate, -bis(ethoxo)bis(thiocyanato)dicopper(II), and -bis(acetonitrile)-bis(methoxo)dicopper(II).

Supplementary data available: see Instructions for Authors, *J. Chem. Soc., Dalton Trans.*, 1988, Issue 1, pp. xvii—xx.
Non-S.I. units employed: cal = 4.184 J, G = 10^{-4} T.

Table 1. Infrared, conductivity, and analytical data for dicopper(II) complexes

Compound	Colour	Analysis (%)[a] N	C	H	Conductivity Λ^b/S cm^2 mol^{-1}	Infrared data (cm^{-1}) ν_{CN}	$\nu_{ClO_4^-}$ or ν_{NCS^-}	$\nu_{BPh_4^-}$	ν_{OR^-}
(1) $[Cu_2(L^1)(pz)_2][ClO_4]_2$	Brownish green	14.3 (14.3)	36.7 (36.7)	3.4 (3.3)	284	1 646s	1 090vs, br	623m	
(2) $[Cu_2(L^1)(dmpz)_2][ClO_4]_2 \cdot H_2O$	Light green	13.1 (13.3)	40.1 (40.0)	4.0 (4.1)	294	1 640s	1 090vs, br	625m	
(3) $[Cu_2(L^1)(trz)_2][ClO_4]_2$	Brown	17.7 (17.8)	33.4 (33.6)	2.9 (3.1)	298	1 640s	1 090vs, br	623m	
(4) $[Cu_2(L^2)(dmpz)_2][ClO_4]_2$	Gold	12.5 (12.4)	42.2 (42.6)	5.6 (5.4)	219	1 638s	1 090vs, br	628m	
(5) $Cu_2(L^1)(OMe)_2(NCS)_2$	Bright green	13.4 (13.3)	41.8 (41.9)	4.0 (3.8)	Insoluble	1 630s	2 105vs	805m	2 797m
(6) $Cu_2(L^1)(OEt)_2(NCS)_2$	Bright green	13.0 (12.8)	43.6 (43.8)	4.4 (4.3)	Insoluble	1 630s	2 090vs	805m	2 849m
(7) $[Cu_2(L^1)(OMe)_2(MeCN)_2][BPh_4]_2$	Bright green	6.8 (6.8)	70.0 (70.1)	5.8 (5.8)	219	1 640(s)	735, 705s		2 787mw
(8) $Cu_2(L^1)(OEt)_2(MeCN)_2(BPh_4)_2$	Green[c]	6.8 (6.7)	71.9 (72.3)	6.4 (6.4)	231	1 640(s)	730, 710s		2 852m
(9) $Cu_2(L^1)(OH)_2(ClO_4)_2 \cdot H_2O$	Green	7.7 (8.0)	31.2 (30.8)	3.7 (3.4)	260	1 635(s)	1 085vs, br	620m	3 500m, br 3 300mw, br
(10) $Cu_2(L^3)(OH)_2(ClO_4)_2$	Brown	7.1 (7.2)	33.9 (34.2)	4.1 (3.9)	Insoluble	1 630(s)	1 090vs, br	625m	3 460m

[a] Calculated values in parentheses. [b] 10^{-3} mol dm^{-3} in MeCN. [c] Rapidly turns brown on standing.

Table 2. Electronic, spectral, and magnetic data for dicopper(II) complexes

Compound	$\lambda_{max.}$[a]/cm^{-1}(ε[b])	$\mu_{eff.}$[c] 293 K	93 K	J/cm^{-1}	g	N_α/c.g.s.u. × 10^{-6}
(1)	33 000(38 000), 28 500 sh, 20 000(154), 16 300(90)	1.42	0.49	−135	2.10	60
(2)	33 300(38 000), 27 800 br sh, 20 000(240), 16 130(125)	1.51	0.57	−137	2.16	160
(3)	32 800(32 000), 29 000 sh, 19 160(170), 16 670(100)	1.73	1.07	−123	2.16	60
(4)	31 250(50 000), 28 170 sh, 20 410(400), 15 970(105)	1.40	0.45	−165	2.14	60
(5)	32 260[d], 25 000 sh[d], 14 000[d], 9 500[d]	1.09	0.34	−250	2.15	120
(6)	32 260[d], 25 000 sh[d], 13 900[d], 9 700[d]	0.83	0.25	−332	2.14	90
(7)	33 300(30 000), 14 000 sh, 9 600 sh 33 000[d], 14 300[d], 9 100[c] brsh	1.20	0.55	−215	2.14	160
(8)	34 000(33 000), 13 900 sh, 9 800 sh		[e]			
(9)	34 720(31 210), 25 640 sh, 20 410(500), 15 150(138)	1.37	0.72	[f]		
(10)	33 000[d], 25 500 sh, 19 500 sh, 15 400 wsh	1.36	0.72	[f]		

[a] In MeCN solution. [b] ε in dm^3 mol^{-1} cm^{-1}. [c] Per Cu^{2+} ion. [d] Nujol mull spectrum. [e] Not measured because of decomposition. [f] Did not fit equation (1).

occurrence of cyclic (2 + 2) Schiff-base condensation has already been established for L^1 and L^2 by *X*-ray crystallographic structure determination.[2-7] We were not able to demonstrate formation of the L^3 macrocycle on Group 2 metal ions; however it formed easily in the presence of Cu^{II}, though this may not represent a true template reaction so much as the 'fixing' by co-ordination of a compound which would otherwise react further to give polymeric material.

Transmetallation of the barium complexes of L^1 and L^2 with excess of copper(II) salt in the presence of bridging ligand yielded the desired dicopper complex. Preparative details are given in the Experimental section.

Characterisation of the Complexes.—The complexes studied are listed in Table 1 together with analytical and selected physical data. The conductivity is in all cases that of a 1:2 electrolyte, showing that the ionic bridge is retained in acetonitrile solution. Infrared spectra show that the integrity of the macrocyclic structure is preserved on transmetallation; there are no $\nu_{C=O}$ or ν_{NH_2} absorptions to suggest ring-opening reactions.

None of the complexes formulated as pyrazolate or 1,2,4-triazolate shows infrared absorptions in the characteristic ν_{NH} stretching region around 3 300—3 400 cm^{-1}, the absence of this absorption confirming the deprotonation of the heterocyclic bridging ligand. A strong broad ν_{OH} absorption at around 3 200—3 500 cm^{-1} characterises the hydroxo-bridged complexes (**9**) and (**10**) while a sharp peak at *ca.* 2 790 cm^{-1} identifies the OMe^- anion in (**5**) and (**7**). The ethoxy anion does not show such characteristic absorption resolvable from ligand ν_{CH} stretches but intensification of a *ca.* 2 850 cm^{-1} peak in (**6**) and (**8**) is presumably due to the presence of this ion. In any case, *X*-ray crystallographic structure determination of (**6**) has shown unambiguously that an ethoxy bridge is present in this dicopper(II) complex, together with terminally *N*-co-ordinated thiocyanate. As expected, ν_{asym}(NCS) appears at high intensity close to 2 090 cm^{-1} in (**5**) and (**6**) and the ν_{sym}(NCS) absorption can probably be assigned to a medium-weak band appearing close to 800 cm^{-1}.

Electronic Spectra.—Electronic spectra of the complexes in acetonitrile solution, or as Nujol mulls where solubility is inadequate, were recorded in the range 30 000—5 000 cm^{-1} (Table 2). The alkoxo- and hydroxo-bridged complexes [with the exception of the L^3 complex (**10**)] are bright green, indicating the absence from the visible region of absorption due to other than *d–d* transitions. The diaza-bridged complexes on the other hand are brown to brownish green owing to ligand to metal charge transfer (l.m.c.t.) absorption of moderate intensity which tails into the visible. The *d–d* spectra of these diaza-bridged complexes (**1**)—(**4**) are basically similar, suggesting that the copper co-ordination geometry is unchanged over this series. The spectra consist of a pair of medium intensity absorptions around 16 000 and 20 000 cm^{-1}. As square-planar Cu^{II} co-ordination is demonstrated (see later) in the *X*-ray crystallographic structure determination of (**1**), these absorptions are assigned, respectively, to the $B_{2g} \rightarrow B_{1g}$ and $E_g \rightarrow B_{2g}$ transitions in D_{4h} symmetry. The charge transfer absorptions are not well resolved from the ligand π–π^* absorption, but are seen as shoulders around 28 000—29 000 cm^{-1} on its wings. L.m.c.t. absorption of this frequency has been observed[8] for a range of Cu^{II} imidazole and pyrazole complexes, so the transition energy appears to be insensitive to the development of charge on the deprotonated ligand.

X-Ray crystallographic structure determinations of $[Cu_2(L^1)(OEt)_2(NCS)_2]$ (**6**) and $[Cu_2(L^1)(OMe)_2(MeCN)_2][BPh_4]_2$ (**7**) reported in the present work* show similar copper(II) co-ordination geometries approximating to trigonal bipyramidal. The electronic spectra of these two compounds are similar, consisting of a pair of *d–d* bands at *ca.* 14 000 cm^{-1} and *ca.* 10 000 cm^{-1}, corresponding respectively to the $2A' \longrightarrow 2E''$ and $2A' \longrightarrow 2E'$ transitions in D_{3h} symmetry. The spectrum for (**7**) is barely altered on going to acetonitrile solution, showing that the alkoxo-bridge is retained in solution. The very broad *d–d* bands in (**7**) and (**8**) overlap with broad intense ligand absorption without resolution of separate components corresponding to $O \rightarrow Cu^{II}$ l.m.c.t., although such absorption is to be expected[9] in the 25 000—28 000 cm^{-1} region. In the thiocyanato complexes (**5**) and (**6**), absorption of moderate intensity is seen as a broad shoulder above 25 000 cm^{-1} arising from the expected[10] $NCS^- \rightarrow Cu^{II}$ l.m.c.t. Complexes (**5**) and (**8**) in fact show electronic spectra so similar to the structurally characterised compounds (**6**) and (**7**) that their co-ordination geometry may also be inferred to be trigonal bipyramidal. The dihydroxo-bridged complexes (**9**) and (**10**) have an electronic spectrum quite different from the alkoxo-bridged dimers, and similar to that generated by the square-planar geometry of complexes (**1**)—(**4**). (The spectrum is not incompatible, however, with weak axial co-ordination of water.) The pair of medium-intensity bands around 15 000 and 20 000 cm^{-1} are attributed to *d–d* transitions, and a poorly resolved shoulder round 25 000 cm^{-1} to $O_{2p} \rightarrow Cu^{II}$ charge transfer.

Crystal Structures of $[Cu_2(L^1)(pz)_2][ClO_4]_2$ (**1**), $[Cu_2(L^1)(OEt)_2(NCS)_2]$ (**6**), *and* $[Cu_2(L^1)(OMe)_2(MeCN)_2][BPh_4]_2$ (**7**).—The structure of the cation of (**1**), $[Cu_2(L^1)(pz)_2][ClO_4]_2$ (pz = pyrazolate) is shown in Figure 1 together with the atomic numbering system. Each copper atom is in a square-planar environment being bonded to two nitrogen atoms from the macrocycle and to two bridging pyrazolate anions. The co-ordination spheres and the bridge are shown more clearly in Figure 2. The perchlorate anions are weakly attracted to the copper atoms in approximately axial positions at distances of 2.761(15) Å [Cu(2)–O(13″)] and 2.527(8) Å [Cu(1)–O(21′)] but we do not consider these to represent bonds. Each copper atom deviates slightly from the plane of its donor N_4 atoms by 0.07 Å for Cu(1) and 0.05 Å for Cu(2). In both cases the atoms that make up the N_4 planes are coplanar to within experimental error.

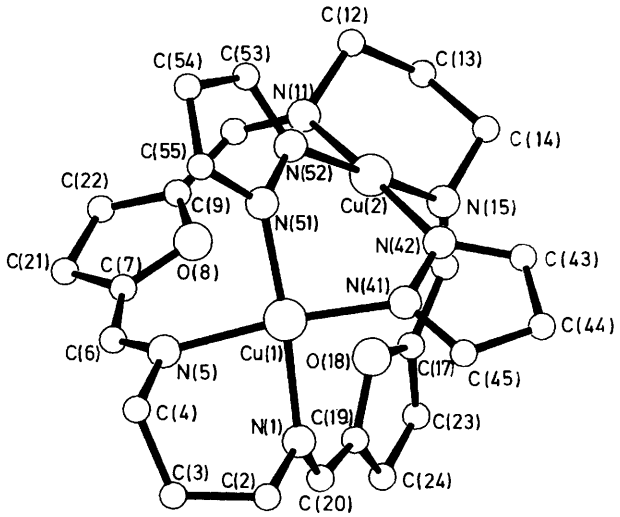

Figure 1. Structure of the cation $[Cu_2(L^1)(pz)_2]^{2+}$ (**1**), showing the atomic numbering scheme

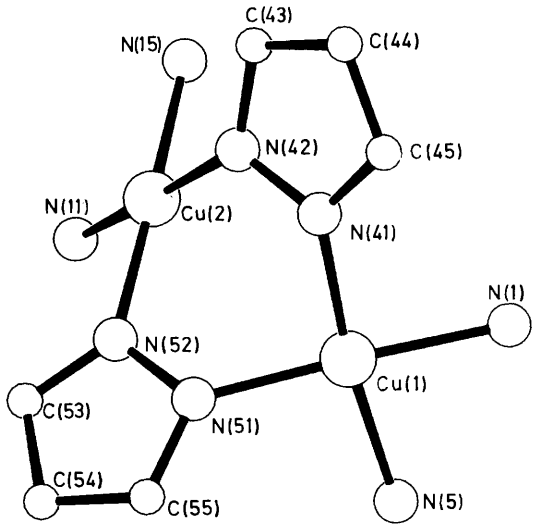

Figure 2. The square-planar copper(II) co-ordination spheres in (**1**)

The two N_4 planes however intersect at an angle of 85.1° (Figure 2). This large angle is due to the steric constraints induced by the bridging pyrazolates. These five-membered rings are themselves planar and intersect each other at an angle of 34.8°. The rings are tilted out of the copper equatorial planes so that one ring, numbered 4, intersects the two N_4 planes at angles of 44.0 and 46.0° respectively while the other ring, numbered 5, intersects the two copper planes at angles of 50.7 and 40.5°. The Cu–N(macrocycle) distances $Cu–N_{av.}$ 2.020 Å are longer than the Cu–N(pyrazolate) distances $Cu–N_{av.}$ 1.950 Å.

The Cu(1)–Cu(2) distance is 3.396(1) Å. This distance between two Cu^{II} centres is considerably longer than the distance found in a comparable Cu^I compound $[Cu_2(L^2)(pydz)_2]^{2+}$ (**11**)[6] (pydz = pyridazine) where the Cu ··· Cu distance is only 3.15 Å.

* A preliminary report of the structure of complex (**6**) has been published.[2]

There have been many binuclear complexes of L^1 and L^2 studied by *X*-ray crystallography. A full list is given in ref. 11. All of these compounds include the two metal atoms each bonded to two nitrogen atoms of the macrocycle in the same fashion as in (**1**). In most of these complexes there are one or two bridges (of one, two, or three atoms) between the metal atoms. The macrocycle is flexible and permits metal–metal distances ranging from 2.80 Å in $[Cu_2(L^1)(NCS)_2]$[3] where the copper atoms are bridged by two sulphur atoms of the bridging thiocyanates, to 3.39 Å in $[Cu_2(L^1)(MeCN)_2]^{2+}$[2] where the copper atoms are only three-co-ordinate bonded to terminal methyl cyanide.

Complex (**1**) contains a similarly long Cu ··· Cu distance of 3.396(1) Å. We have shown elsewhere[11] by molecular mechanics calculations that this relatively long distance is a consequence of steric effects. Thus, for complexes with two two-atom bridges, we have plotted conformational energy of the macrocycle against various fixed Cu ··· Cu distances and geometries and shown that the lowest energy conformation of the complex occurs at a higher energy and a larger Cu ··· Cu distance for the square-planar dinuclear complex (**1**) (36.9 kcal mol^{-1}, 3.45 Å) than for the tetrahedral dinuclear complex (**11**) (33.4 kcal mol^{-1}, 3.30 Å).

The conformations of the macrocycle with square-planar copper(II) and tetrahedral copper(I) are very different. In the tetrahedral case, (**11**), the two copper atoms are coplanar with the plane of the four macrocycle nitrogen atoms and the furan rings are almost parallel (angles of intersection 8.2°) with this N_4 plane, while in the square-planar case (**1**), the two copper atoms are displaced to the same side of the N_4 plane at distances of 1.09, 1.06 Å and the two furan rings make angles of 50.1 and 53.0° respectively with the N_4 plane. It is interesting that the two Cu–N–N–Cu torsion angles are −5.2, 10.0° in (**1**) but 25.0, −25.0° in (**11**). The pyridazine rings in (**11**) are parallel, contrasting with the 34.8° between the pyrazolate rings in (**1**).

The structure of (**6**) is shown in Figure 3 together with the atomic numbering scheme. The structure of (**7**) is similar. Both structures contain the metal atom in an approximately trigonal-bipyramidal environment. In the two structures the differences between comparable angles in the co-ordination sphere are all less than 6.5°.

Both structures contain a crystallographic centre of symmetry and the two copper atoms are bridged *via* two alkoxide groups [ethyl in (**6**) and methyl in (**7**)]. One of the oxygens O(1) is in an axial position *trans* to the monodentate ligand [NCS^- in (**6**) and NCMe in (**7**)]. The other oxygen O(1′) makes up the equatorial plane together with two nitrogen atoms of the macrocycle. These two nitrogen atoms are however non-equivalent and in both structures N(11) is more strongly bound to the metal than N(17′), bond lengths differing by 0.18 Å in both structures. There is also some distortion in the angles in the equatorial plane N(11)–Cu(1)–O(1′) being 140.9(6) in (**6**) and 141.4(11)° in (**7**) compared with N(17′)–Cu(1)–O(1′) values of 121.5(6) and 127.9(15)° respectively. This is indicative of a slight distortion towards a square-planar structure.

The Cu ··· Cu distances in the two structures are 3.003(3) and 2.970(7) Å. This value is considerably less than that found[4] in the similar cobalt compounds $[Co_2(L^1)(OEt)(NCS)_3]$ 3.119 and $[Co_2(L^1)(OMe)(N_3)_3]$ 3.195 Å. Molecular mechanics calculations[11] show that for binuclear molecules with two one-atom bridges within the macrocycle L^1, the trigonal-bipyramidal geometry has a much lower energy (by *ca.* 10.0 kcal mol^{-1}) than either the square-planar or the tetrahedral geometry. This difference is mainly due to a decrease in bending strain at the metal atom and a small number of significant van der Waals 1,4-interactions.

In all four five-co-ordinate structures established by *X*-ray crystallography, the geometry of the complex is the same. The

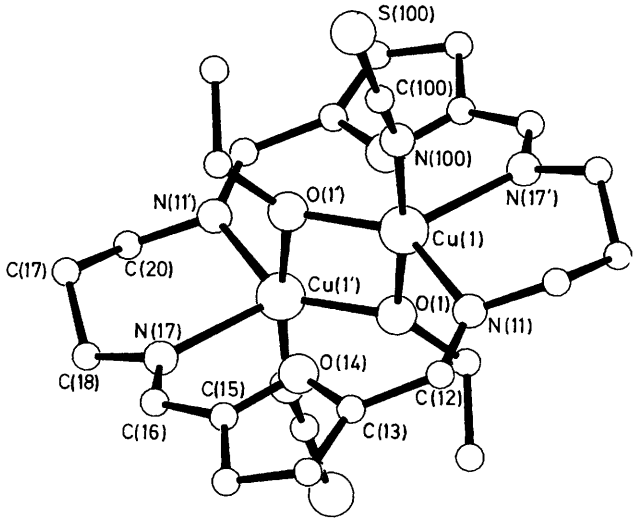

Figure 3. Structure of $[Cu_2(L^1)(OEt)_2(NCS)_2]$, (**6**), showing the atomic numbering scheme

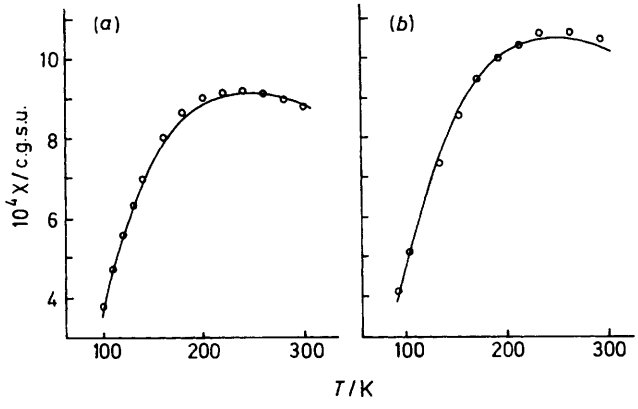

Figure 4. Magnetic susceptibility temperature variation for (*a*) $[Cu_2(L^1)(pz)_2][ClO_4]_2$ and (*b*) $[Cu_2(L^1)(dmpz)_2][ClO_4]_2$ (experimental = ○, theoretical = ——)

M_2X_2 (M = Co or Cu; X = O or N) bridge is perforce planar and the furan rings are approximately parallel to the plane of the four macrocycle nitrogen atoms [angles of intersection 8.0° in (**6**) and 6.2° in (**7**)]. The metal atoms are displaced on opposite sides of the N_4 plane [±0.58 in (**6**), ±0.53 Å in (**7**)].

Magnetic Properties of the Dicopper Complexes.—Measurements of magnetic susceptibility were made by the Gouy method over the temperature range 93—293 K. All the complexes showed some degree of antiferromagnetic interaction, having subnormal room-temperature moments, which reduced further on cooling. The theoretical equation[12] describing the temperature variation of susceptibility for exchange-coupled pairs of $s = \frac{1}{2}$ ions is given as equation (1). The experimental

$$\chi_m = \frac{N\beta^2 g^2}{3kT}[1 + \tfrac{1}{3}\exp(-2J/kT)]^{-1} + N_\alpha \qquad (1)$$

susceptibility *vs.* temperature data were fitted to this equation, where possible, giving the values of *J*, *g*, and N_α listed in Table 2; Figure 4 compares the experimental and calculated χ_m *vs.* *T* curves for diaza-bridged dimers (**1**) and (**2**). Reasonably good

Table 3. Bridging geometry in dicopper(II) complexes (X = bridging ligand) (distances in Å, angles in °)

Compound	Co-ordination geometry	r(Cu ··· Cu)	r(Cu ··· N_{macro})	r(Cu ··· X)	Cu–X–Cu	L_{ax}–Cu–L_{ax}	L_{ax}–Cu–L_{eq}
(**1**)	Square planar	3.396(1)	2.00—2.03	1.94, 1.95			
(**7**)	Trigonal bipyramidal	2.970(7)	2.06—2.23	1.76, 2.07	101	173.5	79—95
(**6**)	Trigonal bipyramidal	3.003(3)	2.10—2.29	1.90, 1.96	102	173.7	78—96

agreement was obtained for the diaza-bridged dimers and for the alkoxo-bridged dimers within the relatively higher error limits associated with their low χ_m values, but the hydroxo-bridged dimers, (**9**) and (**10**), do not conform to equation (1). Below 173 K, the product χT falls off less steeply than expected on the basis of behaviour in the 173—273 K range. One possible explanation is the existence of inter-dimer exchange; the likely 'roof shaped' dimer conformation would leave the bridging hydroxyl groups suitably placed for additional weak interaction with neighbouring copper(II) ions. However, e.s.r. spectra (see later) suggest the presence of paramagnetic impurity, which could make an important contribution to the susceptibility at low temperature.

The strongly reduced paramagnetic susceptibility of the alkoxo-bridged dimers shows that sizeable antiferromagnetic coupling is mediated by their single-atom bridge. Such efficient superexchange is unexpected in this approximate D_{3h} symmetry, given that d_{z^2} is the magnetic orbital, and that the axial bonds from the pair of Cu^{2+} ions run approximately parallel to each other. This makes it difficult, on the Kahn model,[13] to envisage an effective overlap pathway encompassing both magnetic orbitals and the O 2*p* orbitals. Each alkoxo oxygen in the structurally characterised complexes (**6**) and (**7**) occupies an axial/equatorial position with respect to the pair of Cu^{2+} ions. So, although there is excellent overlap with the magnetic orbital on one Cu^{2+} ion in the axial direction, overlap with the magnetic orbital on the second Cu^{2+} ion is poor because the O atom is equatorially positioned relative to that ion. In other structures[14] of the paired trigonal-bipyramidal or parallel-planar type the singlet-triplet splitting $-2J$ is normally small. This is in contrast to the situation in square-based coplanar or 'roof-shaped' dimers where the splitting, $2J$, can attain large negative values for suitable values of the bridging angle Cu–X–Cu. For example, in carboxylate oxygen bridged dimer $[\{Cu[O_2CCH_2NHC(O)Ph]_2\}_2]\cdot 4H_2O$ of the parallel planar type[15] the singlet–triplet splitting $2J$ is only -4.3 cm^{-1} for a Cu–O–Cu angle of 101°. When this angle approaches 90° in the parallel-planar structure the *s* and *p* orbitals on the bridging atom become orthogonal to the d_{z^2} magnetic orbital on one copper(II) ion and ferromagnetic interaction results, as has been indicated[16] for dimeric bis(pyridine *N*-oxide)copper(II) nitrate.

The crystallographic results for (**6**) and (**7**) (Table 3) with L_{ax}–Cu–L_{ax} angles of *ca.* 174° and L_{ax}–Cu–L_{eq} angles of 78.0(5)—95.7(6)° in (**6**), and 78.7(11)—94.8(15)° in (**7**) do not indicate significant distortion of the trigonal-bipyramidal structure towards C_{4v} with accompanying delocalisation of the magnetic orbital into the equatorial plane. Presumably, however, even the minor distortion from regular D_{3h} symmetry observed results in some degree of delocalisation.

Whatever the explanation, it is clear that in both alkoxo-bridged, paired, trigonal-bipyramidal dimers (**6**) and (**7**), sizeable antiferromagnetic coupling is mediated through the bridging oxygen. It is also clear that increased σ donation from the alkyl substituent on to the bridging oxygen enhances the antiferromagnetic interaction, as predicted on theoretical considerations by Hay *et al.*[17] and observed in several laboratories.[18]

The *X*-ray crystallographic structure determination of (**1**) shows that, here, the Cu^{II} co-ordination geometry is essentially square planar, with the bridging N–N link making an angle of *ca.* 120° with the co-ordination plane. In square-planar geometry the magnetic orbital for Cu^{II} is $d_{x^2-y^2}$. One pair of *cis* positions is occupied by the macrocyclic imino donors and the other pair consists of two N atoms, one from each of the bridging pyrazolate ions. The lone pairs on the pyrazolate nitrogens are well placed for effective overlap with the magnetic orbital, and the interaction is presumably transmitted to the second $d_{x^2-y^2}$ orbital mainly by a σ superexchange pathway as normally proposed.[19] However, it should be noted that in the present case, because of the 45° outward tilt of the pyrazolate rings (see discussion of *X*-ray crystal structure), some overlap of the π orbitals of the heterocyclic bridge with the magnetic orbital is also feasible,[20] and it seems probable that both π- and σ-superexchange pathways contribute.

When magnetic interaction takes place through extended bridging ligands, the antiferromagnetic contribution normally dominates.[21] All the diaza-bridged complexes studied in this work display moderately strong antiferromagnetic interaction. There are not many reports of magnetic behaviour in μ-pyrazolato copper(II) dimers available for comparison. A μ-pyrazolato-dicopper(II) complex of 1,3-bis(salicylideneamino)-propan-2-ol[22] with a similar Cu ··· Cu distance of 3.359 Å has a singlet-triplet splitting, $-2J$, of 120 cm^{-1}, somewhat less than that reported here for (**1**). An apparently planar di-μ-pyrazolato-dicopper dimer of unknown Cu ··· Cu distance[23] has a $-2J$ value much less (at 70 cm^{-1}) than that of (**1**). The more efficient exchange mechanism inferred for diaza-bridged L^1 complexes (**1**)—(**4**) may derive from the suggested π-superexchange pathway.

E.S.R. Spectra.—E.s.r. spectra of the complexes were recorded as polycrystalline samples or as frozen glasses in dimethylformamide (dmf) (Table 4). Where there was an indication of decomposition in the frozen solution spectrum, we were in some cases able to prepare the complexes with a tetraphenylborate counter ion in order to introduce sufficient magnetic dilution to allow observation of hyperfine structure.

All the diaza-bridged complexes (**1**)—(**4**) show clear evidence in their e.s.r. spectra of interaction between the paramagnetic centres leading to a ground singlet and excited triplet state. The forbidden $\Delta m = 2$ half-band transition was observed in all cases at 10^{-1}—10^{-2} times the intensity of the $\Delta m = 1$ transition. Even in the polycrystalline spectra, traces of hyperfine splitting could be seen on the half-band signal. The splitting was of the order of 70—90 G, as anticipated, and at least five of the expected seven hyperfine components could be identified.

The main-band signal for complexes (**1**)—(**4**) was broad (Figure 5), extending over 1 000—1 500 G and displaying triplet-type anisotropic splitting with at least the two $g_{x,y}$ components apparent in the broad signal. In favourable cases, at least one g_z component was also observable and identifiable

Table 4. E.s.r. parameters for the dicopper(II) complexes

Compound		$\Delta m = 2$ band		$\Delta m = 1$ band				
		Intensity[a]	h.f.s.[b]	$D_{x,y}$[b]	$g_\perp$	$A_\parallel$[b]	D_z[b]	$g_\parallel$
(1) $[Cu_2(L^1)(pz)_2][BPh_4]_2$	Polycrystalline	$\frac{1}{8}$	95[c]	1 100	2.07	*ca.* 80[c]		
(2) $[Cu_2(L^1)(dmpz)_2][BPh_4]_2$	Polycrystalline	$\frac{1}{7}$	80[c]	1 200	2.09	*ca.* 80[c]		
(3) $[Cu_2(L^1)(trz)_2][ClO_4]_2$	dmf glass	$\frac{1}{20}$	80[c]	720	*ca.* 2.05	70[c]		
(4) $[Cu_2(L^2)(dmpz)_2][ClO_4]_2$	Polycrystalline	$\frac{1}{30}$	85[c]	840	2.08	82[c]	350	2.27
(5) $Cu_2(L^1)(OMe)_2(NCS)_2$	Polycrystalline	*d*		*d*	2.14[e]	*d*		
(6) $Cu_2(L^1)(OEt)_2(NCS)_2$	Polycrystalline	*d*		*d*	2.14[e]	*d*		
(7) $[Cu_2(L^1)(OMe)_2(MeCN)_2][BPh_4]_2$	Polycrystalline	*d*	*d*	200	2.16	*d*	390	2.12
(9) $Cu_2(L^1)(OH)_2(ClO_4)_2 \cdot H_2O$	Polycrystalline	$\frac{1}{1000}$	*ca.* 70[c]	*d*	2.09	74 160[f]	*d*	2.26
(10) $Cu_2(L^3)(OH)_2(ClO_4)_2$	Polycrystalline	*d*	*d*	*d*	2.00	90 180[f]	*d*	*ca.* 2.2

[a] As fraction of $\Delta m = 1$ band. [b] Hyperfine splitting, in Gauss. [c] Poorly resolved, confirmed by 2nd harmonic spectra. [d] Not observed. [e] $g_{av.}$ (one broad signal). [f] Two superimposed hyperfine patterns are seen.

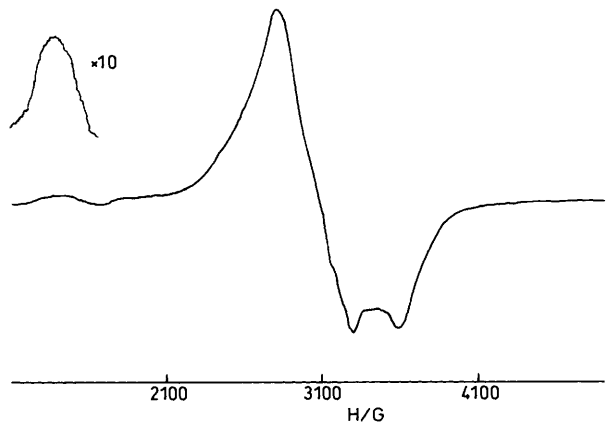

Figure 5. E.s.r. spectrum of polycrystalline $[Cu_2(L^2)(dmpz)_2][ClO_4]_2$ at 93 K

by its hyperfine structure. The hyperfine coupling constant $A_\parallel$ is similar to that appearing in the $\Delta m = 2$ signal. Values of the zero-field splitting parameter $D_{x,y}$ can be estimated from the spectra, but serious overlapping problems in most cases prevent even approximate evaluation of D_z or $g_\parallel$. The value of $D_{x,y}$ varies from $>1\,000$ G in the di-μ-pyrazolato complex (**1**) to *ca.* 700 G in the di-μ-triazolato complex (**3**), *i.e.* roughly (but possibly coincidentally) in line with the trend in the magnetic exchange parameter, $-2J$. The internuclear distance revealed in the *X*-ray crystallographic structure determination of (**1**) suggests[24] a dipolar contribution to zero-field splitting, D_{dip} of *ca.* 0.02 cm^{-1}, *i.e.* significantly less than the observed zero-field splitting. This indicates an appreciable pseudo-dipolar contribution, D_{pseudo}. A value of $D_{pseudo} > D_{dip}$ is explained[24] by excited-state exchange using a π-type superexchange pathway and involving for example d_{xy}–π* electron exchange. As we have noted earlier, the tilt of the pyrazolate rings in (**1**) relative to the copper equatorial planes allows for overlap of pyrazolate π* orbitals with $d_{x^2-y^2}$ or d_{xy} orbitals. This tilt is a parameter which is likely to vary with substitution on the heterocyclic bridge in consequence of mutual repulsion between these *cis* disposed ligands. Alteration of the tilt will affect the efficiency of the π-exchange pathway and hence the value of the pseudo-dipolar contribution, which presumably explains the range of *D* values obtained with these otherwise very similar complexes. As the Cu ••• Cu distance is not expected to vary much over the series (**1**)—(**4**), D_{dip} is not expected to alter with the nature of the heterocyclic bridge.

As befits its strongly reduced magnetic susceptibility, the ethoxy-bridged complex (**6**) shows only a weak, broad, room-temperature signal, being e.s.r. silent at 93 K. The methoxy-bridged complexes (**5**) and (**7**) are also e.s.r. silent at 93 K but show a medium–weak room-temperature signal, which for (**5**) is broad and structureless. In the more magnetically dilute compound (**7**) greater zero-field splitting is seen in the 'parallel' components, D_z, than in the 'perpendicular' $D_{x,y}$ components. This is to be expected in the paired trigonal-bipyramidal structure typified by (**6**) and (**7**) where interaction is confined to within the Cu_2O_2 plane, negligible interaction being present along the axis perpendicular to this plane. Using the crystallographically obtained data, a value of around 0.025 cm^{-1} is calculated, in fair agreement with the average of the observed $D_\perp$ and $D_\parallel$ splittings. There seems to be no need to invoke a pseudo-dipolar contribution to zero-field splitting in these compounds.

The e.s.r. spectra of the μ-hydroxo-bridged dimers are quite different in appearance from the diaza-bridged dimers despite their reasonably similar room-temperature magnetic susceptibilities and electronic spectra which suggest square-planar Cu^{II} in this, as in the diaza-bridged series. The Cu ••• Cu distances are not expected to exceed the 3.39 Å separation existing in (**1**) they may indeed be appreciably shorter, along the lines of the 3.145 Å separation observed[25] for the Cu ••• Cu distance in a μ-hydroxo-bridged dimer of a related ligand. However, apart from reduced signal intensity, the e.s.r. spectra of compounds (**9**) and (**10**) give little evidence of interaction between Cu^{2+} ions. The spectra reveal at best only small zero-field effects; the main-band perpendicular signals are merely broadened, not split. A very weak half-band signal at *ca.* 10^{-3}, the intensity of the $g = 2$ signal is observable for (**9**) at maximum instrumental sensitivity. Poorly resolved hyperfine splitting is just discernible at 93 K on the half-band signal and (more easily) on the low-field wing of the main band of (**9**), where a spacing of *ca.* 75 G, as expected for a dicopper(II) dimer, can be distinguished. This appears to be overlaid in both (**9**) and (**10**) by a second hyperfine pattern with $A_\parallel$ *ca.* 170 G which suggests the presence of a small proportion of non-interacting Cu^{II} arising perhaps from a ring-opening reaction which is known to occur[26] readily in these systems. The lack of any clearly defined zero-field splitting on a dimer where the likely internuclear distance suggests a dipolar contribution in excess of 0.02 cm^{-1} is unexpected. Possibly in this case the pseudo-dipolar contribution opposes rather than enhances D_{dip}.

Conclusions

As expected, by reason of their macrocycle-imposed proximity, the Cu^{2+} ions in all the dimers studied interact, but do so in a very different fashion according to geometry and the nature of the bridging ligand. Thus, the alkoxo bridges in the paired trigonal-bipyramidal dimers are responsible for the largest single–triplet separation, $-2J$, and these dimers are completely in the singlet state at 93 K. This is despite the lack of any obvious superexchange pathway linking the d_{z^2} magnetic orbitals. In consequence of their reduced magnetic susceptibilities, the dimers are e.s.r. silent at 93 K but can show weak triplet spectra at 293 K, with zero-field splitting of much the same magnitude as predicted on a dipolar coupling model.

The diaza-bridged dimers show only moderate antiferromagnetic exchange, but sizeable zero-field splitting in their triplet e.s.r. spectra which are observed at all temperatures in the 93—293 K range, but are more clearly resolved at low temperature. The size of the zero-field splitting suggests that a pseudo-dipolar contribution is important, involving an excited-state π-superexchange pathway. The hydroxo-bridged dimers do not show any significant zero-field splitting effects in their e.s.r. spectra, and their magnetic behaviour is complex, arising either from interdimer exchange and/or the presence of paramagnetic impurity deriving from ring-opening reactions.

Experimental

Preparation of the Ligands.—The ligands L^1 and L^2 were prepared as their Ba^{2+} or Ca^{2+} complexes, by template synthesis, from 2,5-diformylfuran and the appropriate diamine as described earlier.[6] The ligand L^3 was not formed either as a Group 2 metal salt or as free ligand in the absence of template. It was obtained by Schiff-base condensation in the presence of Cu^{2+}, as described below.

Preparation of the Complexes.—$Cu_2(L^1)(OH)_2(ClO_4)_2\cdot H_2O$. $[Ba(L^1)(ClO_4)_2]\cdot EtOH$ was transmetallated in ethanol solutions, with a slight excess of $Cu(ClO_4)_2\cdot 6H_2O$, as described elsewhere.[6] An analogous procedure with $[Ca(L^2)(ClO_4)_2]\cdot EtOH$ did not result in the isolation of a solid dicopper(II) complex, although u.v. spectral changes suggest that such a complex may be present in solution. (Presumably high solubility in alcohol prevented its isolation in a pure form.)

$Cu_2(L^3)(OH)_2(ClO_4)_2$. 2,5-Diformylthiophene (3.4 mmol) was dissolved in the minimum quantity of a 1:2 ethanol–acetonitrile solvent mixture. 2,2′-Dimethyldiaminopropane (3.1 mmol) was dissolved in ethanol (5 cm^3) and then added to the reaction mixture which was heated at 50 °C for 30 min. $Cu(ClO_4)_2\cdot 6H_2O$ (2.15 mmol) in ethanol (5 cm^3) was added and heating was continued for a further 2 h. The brown product separated out and was filtered off in 30% yield. This product was highly insoluble in all solvents tried, which prevented its conversion to other μ-alkoxo or μ-pyrazolato dimers, for example.

$Cu_2(L^1)(X)_2(ClO_4)_2$ [X = *pyrazolate* (pz), 3,5-*dimethylpyrazolate* (dmpz), *or* 1,2,4-triazolate (trz)]. To a hot solution of $Cu_2(L^1)(OH)_2(ClO_4)_2\cdot H_2O$ (1.2 mmol) in an acetonitrile–ethanol (1:1) solvent (200 cm^3) was added excess of a solution of the heterocycle dissolved in the minimum quantity of ethanol. The resulting greenish brown solution was concentrated and the product crystallised out on standing in 65—70% yield.

$[Cu_2(L^2)(dmpz)_2][ClO_4]_2$. To a solution of $[Ca(L^2)(ClO_4)_2]\cdot EtOH$ (1 mmol) in MeCN (5 cm^3) was added $Cu(ClO_4)_2\cdot 6H_2O$ (2 mmol) and then 3,5-dimethylpyrazole (2.5 mmol) in ethanol (2 cm^3). After 3 h at room temperature, the light gold product crystallised out in 65% yield.

$Cu_2(L^1)(OR)_2(NCS)_2$ (R = Me *or* Et). $Cu_2(L^1)(OH)_2(ClO_4)_2\cdot H_2O$ (0.5 mmol) was dissolved in an ethanol–acetonitrile (1:1) mixture (40 cm^3) and stirred at room temperature. On addition of Na(NCS) (1.2 mmol) in ethanol (10 cm^3), a bright green precipitate was obtained in 70—80% yield.

$[Cu_2(L^1)(OR)_2(MeCN)_2][BPh_4]_2$ (R = Me *or* Et). $Cu_2(L^1)(OH)_2(ClO_4)_2\cdot H_2O$ (0.5 mmol) was dissolved in a dried ethanol–acetonitrile (3:1) solvent mixture (40 cm^3) and cooled in an ice–salt bath. $Na(BPh_4)$ (0.7 mmol) was dissolved in dry alcohol (10 cm^3), cooled to −15 °C, and added to the dicopper(II) solution. The product crystallised out in 40—50% yield on addition of dry diethyl ether (5 cm^3) and leaving in the

Table 5. Atomic co-ordinates (× 10^4) for complex (**1**) with, estimated standard deviations (e.s.d.s) in parentheses

Atom	*x*	*y*	*z*	Atom	*x*	*y*	*z*
Cu(1)	6 991(0)	639(1)	−21(1)	C(22)	6 282(5)	−885(10)	2 759(6)
Cu(2)	8 055(0)	−1 634(1)	1 387(1)	C(23)	9 080(5)	1 998(9)	3 213(6)
N(1)	7 234(3)	2 481(6)	251(5)	C(24)	8 647(7)	2 941(9)	2 635(7)
C(2)	6 774(4)	3 340(7)	−497(6)	N(41)	7 972(3)	294(6)	24(4)
C(3)	6 004(4)	3 388(7)	−503(6)	N(42)	8 398(3)	−660(5)	558(4)
C(4)	5 625(4)	2 122(8)	−681(5)	C(45)	8 400(5)	999(8)	−265(6)
N(5)	6 036(3)	1 210(5)	46(4)	C(44)	9 119(4)	544(8)	70(7)
C(6)	5 815(4)	1 078(8)	724(6)	C(43)	9 077(5)	−501(8)	592(6)
C(7)	6 114(4)	280(8)	1 508(5)	N(51)	6 703(3)	−1 132(5)	−179(4)
O(8)	6 704(3)	−488(5)	1 649(3)	N(52)	7 101(3)	−2 013(5)	437(4)
C(9)	6 791(5)	−1 211(8)	2 396(6)	C(54)	5 993(4)	−2 841(8)	−347(6)
C(10)	7 320(5)	−2 207(7)	2 716(5)	C(53)	6 676(5)	−3 047(7)	333(6)
N(11)	7 774(4)	−2 508(6)	2 366(4)	C(55)	6 042(4)	−1 641(8)	−662(6)
C(12)	8 253(6)	−3 609(8)	2 774(7)	Cl(2)	6 205(1)	4 359(2)	2 288(2)
C(13)	9 041(5)	−3 224(8)	3 377(7)	O(21)	6 576(5)	4 244(9)	3 231(5)
C(14)	9 424(6)	−2 440(8)	2 899(8)	O(22)	5 756(9)	3 367(14)	1 996(9)
N(15)	8 987(4)	−1 293(6)	2 485(5)	O(23)	6 631(7)	4 516(16)	1 812(8)
C(16)	9 171(5)	−304(8)	2 972(6)	O(24)	5 791(11)	5 428(23)	2 166(14)
C(17)	8 862(5)	915(8)	2 729(5)	Cl(1)	1 258(1)	4 470(2)	−298(2)
O(18)	8 290(3)	1 127(4)	1 888(3)	O(11)	1 834(7)	4 466(17)	598(9)
C(19)	8 168(5)	2 411(7)	1 824(6)	O(12)	641(5)	3 828(10)	−272(8)
C(20)	7 657(4)	3 014(7)	1 013(5)	O(13)	1 557(7)	3 888(13)	−851(10)
C(21)	5 850(5)	51(10)	2 193(6)	O(14)	1 065(7)	5 640(10)	−643(13)

freezer for 2—3 d. The ethoxy-derivative decomposed readily at room temperature in the absence of solvent, which prevented accurate determination of its magnetic properties.

X-Ray Crystal Structure Determination.—Crystals of complexes (**1**), (**6**), and (**7**) were prepared as described above.

Crystal data for (**1**). $C_{24}H_{26}Cl_2Cu_2N_8O_{10}$, M = 783.5, monoclinic, a = 19.680(8), b = 10.660(13), c = 15.558(9) Å, β = 112.5(1)°, U = 3 015.4 Å^3, Z = 4, D_m = 1.72, D_c = 1.73 g cm^{-3}, $F(000)$ = 1 188, λ(Mo-K_α) = 0.710 7 Å, μ = 17.1 cm^{-1}, space group $P2_1/c$.

Crystal data for (**6**). $C_{24}H_{30}Cu_2N_6S_2$, M = 657.4, monoclinic, a = 15.356(10), b = 10.239(9), c = 18.662(16) Å, β = 102.5(1)°, U = 2 864.7 Å^3, Z = 4, D_m = 1.52, D_c = 1.52 g cm^{-3}, $F(000)$ = 1 352, λ(Mo-K_α) = 0.710 7 Å, μ = 17.2 cm^{-1}, space group $I2/c$.

Crystal data for (**7**). $C_{72}H_{72}B_2Cu_2N_6O_4$, M = 1 234.1, monoclinic, a = 17.697(12), b = 14.830(13), c = 12.237(9) Å, β = 105.0(1)°, U = 3 102.25 Å^3, Z = 2, D_m = 1.28, D_c = 1.28 g cm^{-3}, $F(000)$ = 1 292, λ(Mo-K_α) = 0.710 7 Å, μ = 7.46 cm^{-1}, space group $P2_1/n$.

Crystals of approximate size 0.25 × 0.3 × 0.3 mm for (**1**) and 0.35 × 0.35 × 0.35 mm for (**6**) and (**7**) were set up to rotate about the a axes on a Stoe-Stadi2 diffractometer and data were collected *via* variable-width ω scan. Background counts were for 20 s and a scan rate of 0.0333° s^{-1} was applied to a width of (x + sin μ/tan θ) with x = 2.0 (**1**), 1.5 (**6**), and 1.5 (**7**). For (**1**) 5 598, for (**6**) 1 546, and for (**7**) 2 245 independent reflections were measured of which 3 880 with $I > 3\sigma(I)$ for (**1**), 912 with $I > 1.5\sigma(I)$ for (**6**), and 766 with $I > 1.5\sigma(I)$ for (**7**) were used in subsequent refinement.

Standard reflections were measured every 20 reflections. Maximum 2θ values were 50, 40, 50° respectively for the three structures. No deterioration in the standards was noted for (**1**) and (**6**) but intensities for (**7**) dropped by *ca.* 35% during the data collection. An appropriate linear correction was made. The structures were determined by the heavy-atom method. For (**1**) and (**6**) all non-hydrogen atoms were refined anisotropically but for (**7**) only the copper atoms were so treated. In (**7**) the benzene rings in the $[BPh_4]^-$ anion were treated as rigid groups. In all three structures hydrogen atoms were fixed in trigonal or

Table 6. Atomic co-ordinates (× 10^4) for complex (**6**) with e.s.d.s in parentheses

Atom	x	y	z
Cu(1)	771(2)	−857(3)	5 343(2)
N(11)	1 486(10)	−1 984(16)	4 723(10)
C(12)	1 722(14)	−1 669(23)	4 140(13)
C(13)	1 485(15)	−375(22)	3 753(14)
O(14)	918(8)	456(13)	4 010(7)
C(15)	847(13)	1 465(24)	3 573(11)
C(16)	244(15)	2 574(21)	3 634(11)
N(17)	−331(11)	2 552(18)	4 021(10)
C(18)	−975(13)	3 676(24)	3 969(12)
C(19)	−1 186(17)	4 113(23)	4 672(13)
C(20)	−1 845(17)	3 240(21)	4 951(12)
C(21)	1 753(14)	148(29)	3 176(12)
C(22)	1 304(18)	1 366(29)	3 032(13)
N(100)	1 837(12)	−600(19)	6 112(11)
C(101)	2 542(15)	−273(21)	6 453(12)
S(102)	3 457(4)	232(7)	6 980(3)
O(1)	−299(7)	−912(13)	4 606(7)
C(2)	−804(7)	−2 024(13)	4 255(7)
C(3)	−759(23)	−2 236(32)	3 454(16)

Table 8. Molecular dimensions in the metal co-ordination spheres of complex (**1**); distances (Å), angles (°)

Cu(1)–N(1)	2.027(6)	Cu(2)–N(11)	2.034(8)
Cu(1)–N(5)	2.017(7)	Cu(2)–N(15)	2.004(6)
Cu(1)–N(41)	1.939(7)	Cu(2)–N(42)	1.967(7)
Cu(1)–N(51)	1.960(6)	Cu(2)–N(52)	1.936(5)
Cu(1)–O(21′)	2.527(8)	Cu(2)–O(13″)	2.761(15)
N(1)–Cu(1)–N(5)	81.16(27)	N(11)–Cu(2)–N(15)	82.36(29)
N(1)–Cu(1)–N(41)	91.42(27)	N(11)–Cu(2)–N(42)	173.33(22)
N(5)–Cu(1)–N(41)	171.90(24)	N(15)–Cu(2)–N(42)	91.77(28)
N(1)–Cu(1)–N(51)	173.35(33)	N(11)–Cu(2)–N(52)	90.83(27)
N(5)–Cu(1)–N(51)	93.77(27)	N(15)–Cu(2)–N(52)	172.93(34)
N(41)–Cu(1)–N(51)	93.37(28)	N(42)–Cu(2)–N(52)	94.91(26)

Symmetry elements: ′, x, $\frac{1}{2} - y$, $\frac{1}{2} + z$; ″, $1 - x$, $-y$, $-z$.

Table 7. Atomic co-ordinates (× 10^4) for complex (**7**) with e.s.d.s in parentheses

Atom	x	y	z	Atom	x	y	z
Cu(1)	254(3)	957(3)	−128(3)	C(64)	4 720(11)	383(19)	1 494(17)
O(1)	−175(14)	223(16)	995(21)	C(65)	4 499(11)	1 099(19)	2 248(17)
C(1)	−275(27)	198(32)	2 091(35)	C(66)	3 855(11)	1 011(19)	3 181(17)
N(11)	948(14)	1 588(18)	753(20)	C(71)	2 954(14)	221(15)	5 614(14)
C(12)	1 563(15)	1 282(17)	935(20)	C(72)	3 725(14)	−27(15)	5 547(14)
C(13)	1 811(16)	230(18)	636(20)	C(73)	4 008(14)	7(15)	6 509(14)
O(14)	1 366(13)	−210(14)	183(16)	C(74)	3 520(14)	289(15)	7 539(14)
C(15)	1 826(15)	−1 056(23)	272(21)	C(75)	2 749(14)	537(15)	7 607(14)
C(16)	1 551(23)	−1 749(27)	−236(30)	C(76)	2 466(14)	503(15)	6 644(14)
N(17)	812(18)	−1 825(20)	−339(23)	C(81)	1 995(13)	777(14)	4 376(19)
C(18)	507(19)	−2 846(27)	−761(28)	C(82)	2 099(13)	1 580(14)	3 763(19)
C(19)	82(27)	−2 793(36)	−1 674(43)	C(83)	1 459(13)	2 133(14)	3 780(19)
C(20)	−827(25)	−2 540(32)	−972(38)	C(84)	713(13)	1 883(14)	4 411(19)
C(21)	2 491(19)	0(21)	862(23)	C(85)	609(13)	1 079(14)	5 024(19)
C(22)	2 511(16)	−985(27)	487(21)	C(86)	1 250(13)	526(14)	5 007(19)
N(100)	703(23)	1 591(29)	−1 368(34)	C(91)	2 282(11)	−1 031(13)	4 549(18)
C(100)	1 017(16)	2 074(20)	−2 044(22)	C(92)	1 940(11)	−1 249(13)	3 677(18)
C(101)	1 487(19)	2 752(24)	−3 082(28)	C(93)	1 558(11)	−2 074(13)	3 689(18)
B(1)	2 690(31)	5(36)	4 451(37)	C(94)	1 519(11)	−2 680(13)	4 574(18)
C(61)	3 433(11)	206(19)	3 361(17)	C(95)	1 860(11)	−2 461(13)	5 447(18)
C(62)	3 654(11)	−510(19)	2 608(17)	C(96)	2 242(11)	−1 637(13)	5 434(18)
C(63)	4 298(11)	−422(19)	1 674(17)				

Table 9. Dimensions in the metal co-ordination spheres for complexes (**6**) and (**7**); distances (Å), angles (°)

	(6)	(7)		(6)	(7)
Cu(1)–O(1)	1.903(11)	1.764(25)	Cu(1)–O(1′)	1.961(13)	2.070(25)
Cu(1)–N(11)	2.103(19)	2.056(24)	Cu(1)–N(17′)	2.286(19)	2.232(31)
Cu(1)–N(100)	1.947(17)	1.787(42)	Cu(1)···Cu(1′)	3.003(3)	2.970(7)
O(1)–Cu(1)–N(11)	93.3(6)	93.8(10)	N(11)–Cu(1)–N(100)	91.4(7)	90.7(14)
O(1)–Cu(1)–N(100)	173.7(7)	173.5(15)	N(11)–Cu(1)–O(1′)	140.9(6)	141.4(11)
O(1′)–Cu(1)–N(17′)	121.5(6)	127.9(15)	N(11)–Cu(1)–N(17′)	96.7(6)	100.5(11)
N(11)–Cu(1)–N(100)	91.4(7)	90.7(14)	N(100)–Cu(1)–O(1′)	95.7(6)	94.8(15)
O(1)–Cu(1)–O(1′)	78.0(5)	78.7(11)	N(100)–Cu(1)–N(17′)	90.9(7)	94.3(15)
O(1)–Cu(1)–N(17′)	92.7(6)	89.5(11)			

Symmetry element: ′, $-x,-y,1-z$ in (**6**), $-x,-y,-z$ in (**7**).

tetrahedral positions and given isotropic thermal parameters which were allowed to refine in (**1**) and (**6**) but not in (**7**). The structures were refined by full-matrix least squares to R 0.070 (R' 0.073) for (**1**), R 0.073 (R' 0.075) for (**6**), and R 0.092 (R' 0.106) for (**7**). In the final cycle of refinement, all shift/error ratios were $<0.3\sigma$. The final difference Fourier map showed no peaks greater than 0.7 e Å^{-3}. Calculations were carried out using SHELX 76[27] and some of our own programs on the Amdahl V7 at the University of Reading. Final positional parameters are given in Tables 5, 6, and 7 and bond lengths and angles in Tables 8 and 9.

Additional material available from the Cambridge Crystallographic Data Centre comprises H-atom co-ordinates, thermal parameters, and remaining bond lengths and angles.

Physical Measurements.—Magnetic susceptibility, conductivity, and i.r. spectral measurements were made as described elsewhere.[28] Electronic spectra were obtained as MeCN solutions or Nujol mulls, using a Perkin-Elmer λ9 spectrophotometer. *X*-Band e.s.r. spectra were measured using a Varian E109 spectrometer.

Acknowledgements

We thank the Department Education, Northern Ireland and the S.E.R.C. for support. Acknowledgement is also due to the S.E.R.C. for funds for the diffractometer, λ9 spectrometer, and Varian E109 e.s.r. spectrometer. We thank Mr. A. W. Johans for assistance with the crystallographic investigations.

References

1 D. Fenton, *Inorg. Chim. Acta*, 1982, **62**, 51; M. Mikuriya, H. Okawa, S. Kida, and I. Ineda, *Bull. Chem. Soc. Jpn.*, 1978, **51**, 2920 and refs. therein.
2 M. G. B. Drew, A. Lavery, F. S. Esho, and S. M. Nelson, *J. Am. Chem. Soc.*, 1983, **105**, 5693.
3 S. M. Nelson, F. S. Esho, and M. G. B. Drew, *J. Chem. Soc., Chem. Commun.*, 1981, 388.
4 M. G. B. Drew, F. S. Esho, A. Lavery, and S. M. Nelson, *J. Chem. Soc., Dalton Trans.*, 1984, 545.
5 M. G. B. Drew, P. C. Yates, J. T. Grimshaw, K. P. McKillop, and S. M. Nelson, *J. Chem. Soc., Chem. Commun.*, 1985, 262.
6 M. G. B. Drew, P. C. Yates, J. T. Grimshaw, A. Lavery, K. P. McKillop, S. M. Nelson, and J. Nelson, *J. Chem. Soc., Dalton Trans.*, 1988, 347.
7 M. G. B. Drew, F. S. Esho, and S. M. Nelson, *J. Chem. Soc., Dalton Trans.*, 1983, 1653.
8 H. J. Schugar, in 'Copper Coordination Chemistry: Biochemical and Inorganic Perspectives,' eds. K. D. Karlin and J. Zubieta, Adenine, New York, 1983, pp. 43—74.
9 S. Kida, H. Okawa, and Y. Nishida, in ref. 8 pp. 425—444.
10 P. Day, *Inorg. Chem.*, 1966, **5**, 1619.
11 M. G. B. Drew and P. C. Yates, *J. Chem. Soc., Dalton Trans.*, 1987, 2563.
12 B. Bleaney and K. D. Bowers, *Proc. R. Soc., London, Ser. A*, 1952, **214**, 451.
13 O. Kahn, *Angew. Chem., Int. Ed. Engl.*, 1985, **24**, 834.
14 See, for example, W. E. Hatfield, in 'Magneto-Structural Correlations in Exchange-Coupled Systems,' eds. D. Gatteschi, O. Kahn, and R. D. Willett, D. Reidel, Dordrecht, 1985, pp. 555—602.
15 F. D. Estes, W. E. Estes, R. P. Scaruge, W. E. Hatfield, and D. J. Hodgson, *Inorg. Chem.*, 1975, **14**, 2564.
16 K. T. McGregor, J. A. Barnes, and W. E. Hatfield, *J. Am. Chem. Soc.*, 1973, **95**, 7993.
17 P. J. Hay, J. C. Thibeault, and R. Hoffman, *J. Am. Chem. Soc.*, 1975, **97**, 4884.
18 W. R. McWhinnie, *J. Inorg. Nucl. Chem.*, 1965, **27**, 1271; W. Mazurek, K. J. Berry, K. S. Murray, M. J. O'Connor, M. R. Shaw, and A. C. Wedd, *Inorg. Chem.*, 1982, **21**, 3071; N. F. Curtis, C. R. Clark, B. W. Sketa, and T. N. Walters, *J. Chem. Soc., Dalton Trans.*, 1977, 1051; J. A. Bertrand and C. E. Kirkwood, *Inorg. Chim. Acta*, 1972, **6**, 248.
19 R. Prins, P. J. M. W. L. Birker, J. G. Haasnoot, G. C. Verschoor, and J. Reedijk, *Inorg. Chem.*, 1985, **24**, 4128.
20 M. S. Haddad, D. N. Hendrickson, P. Cannedy, R. S. Drago, and D. S. Bieksta, *J. Am. Chem. Soc.*, 1979, **101**, 898.
21 O. Kahn, in 'Magneto-Structural Correlations in Exchange Coupled Systems,' eds. D. Gatteschi, O. Kahn, and R. D. Willett, D. Reidel, Dordrecht, 1985, pp. 57—85.
22 W. Mazurek, B. J. Kennedy, K. S. Murray, M. J. O'Connor, J. R. Rodgers, H. R. Snow, A. G. Wedd, and P. J. Zwakc, *Inorg. Chem.*, 1985, **24**, 3248.
23 G. G. Barraclough, R. W. Brookes, and R. L. Martin, *Aust. J. Chem.*, 1974, **27**, 1843.
24 T. R. Felthouse and D. R. Hendrickson, *Inorg. Chem.*, 1978, **17**, 444.
25 M. G. B. Drew, J. Nelson, F. S. Esho, V. McKee, and S. M. Nelson, *J. Chem. Soc., Dalton Trans.*, 1982, 1837.
26 J. T. Grimshaw, K. P. McKillop, S. M. Nelson, and J. Nelson, *J. Chem. Soc., Dalton Trans.*, in the press.
27 G. M. Sheldrick, SHELX 76, Program for Crystal Structure Determination, University of Cambridge, 1976.
28 M. G. B. Drew, P. C. Yates, B. P. Murphy, J. Nelson, and S. M. Nelson, *J. Chem. Soc., Dalton Trans.*, 1987, 1001.

Received 30*th December* 1987; *Paper* 7/2273